Time-Delayed Output Feedback Bilateral Teleoperation With Force Estimation for n-DOF Nonlinear Manipulators

John M. Daly and David W. L. Wang, *Member, IEEE*

***Abstract*— This brief presents a novel bilateral teleoperation algorithm for n degree of freedom nonlinear manipulators connected through time delays. Central to this approach is the use of second-order sliding mode unknown input observers for estimating the external forces, removing the need for both velocity and force sensors. This leads to a lower-cost hardware setup that provides all of the advantages of a position-force teleoperation algorithm. Stability is guaranteed considering the presence of time delays. Numerical and experimental results are presented.**

***Index Terms*— Bilateral teleoperation, force estimation, sliding mode control, sliding mode observers, time delays.**

I. Introduction

BILATERAL teleoperation involves the ability to control a remote manipulator and to sense the forces acting on the robot in the remote environment. One of the major issues with time-delayed bilateral teleoperation is that of stability.

Several bilateral teleoperation architectures exist, including the position-position and position-force architectures. An issue with the position-position approach is that differences between the master and slave position may be experienced as large reaction forces by the operator, even when the slave may be operating completely in free motion [1]. Niemeyer and Slotine [2] have developed a well known variant of this architecture based on wave variables and ensuring passivity of the closed loop. The position-force architecture involves transmitting the master position to the slave side and then a measurement of the slave environment force back from the slave to the master side. The advantages of this architecture are perfect force tracking when the slave is in contact with an environment and a better perception of the system in free motion [3].

Polushin *et al.* [4] have recently proposed an approach to bilateral teleoperation for n degree of freedom (DOF) nonlinear manipulators over a network with unknown and varying time delays. It requires the assumption that the environment is a passive operator in order to guarantee stability. Garcia-Valdovinos *et al.* [5] proposed the use of a second-order sliding-mode controller for the slave in a bilateral teleoperation system with a constant but unknown time delay. Linear 1-DOF models of the master and slave dynamics are used. The master manipulator is controlled with a standard impedance controller. Proof of stability is given, but it requires that both the human and the environment be passive in order to show stability [5]. This approach requires force sensors.

This brief presents a novel bilateral teleoperation algorithm for n-DOF nonlinear manipulators that provide the benefits of a position-force architecture in terms of transparency and force tracking, but does not require the use of force sensors. The work presented here extends our earlier work presented in [6] and [7]. The work in [6] was developed for linear 1-DOF systems, while [7] presents our preliminary results for nonlinear n-DOF teleoperation systems. This brief builds upon the results of [7] by extending the closed-loop stability results for both delay-dependent and delay-independent stability, and performing a thorough simulation study.

In Section II, the bilateral teleoperation system, along with associated controllers and observers, is presented. Section III presents the stability analysis of each of the master and slave systems, while Section IV develops stability results for the entire closed loop. Numerical simulations are presented in Section V, and an experimental verification is given in Section VI. Conclusions and areas for future work are given in Section VII.

II. Problem Formulation

Although similar to [8], which deals with linear 1-DOF systems and requires measurement of positions, velocities, and external forces, the algorithm presented here is developed for nonlinear n-DOF manipulators and requires only position measurements. A sliding mode controller is used at the slave side to ensure a desired closed-loop impedance and tracking of the delayed master trajectory. A computed torque method impedance controller at the master side is used to give the master a desired impedance and to apply the reflected slave environment force back to the master. Robot position measurements drive observers that estimate both the state and the external forces. The control algorithm in this brief is designed in the manipulator Cartesian space and the slave environment is modeled as an n-DOF system acting on the slave end effector. In this brief, it is assumed that time delays are constant. Provided that an upper bound on the time delays in the system is known, a buffer may be implemented in software to ensure that incoming signals arrive to the controller at a known constant rate.

Consider the following master manipulator dynamics in task space:

$$\dot{\boldsymbol{X}}_{\boldsymbol{m_1}} = \boldsymbol{X}_{\boldsymbol{m_2}} \tag{1}$$

Manuscript received August 31, 2011; revised September 3, 2012; accepted December 23, 2012. Manuscript received in final form January 19, 2013. Date of publication February 14, 2013; date of current version December 17, 2013. Recommended by Associate Editor M. Fujita.

J. Daly is with JSI Telecom, Kanata, ON K2M 1X3, Canada (e-mail: jmdaly@gmail.com).

D. Wang is with the Department of Electrical and Computer Engineering, University of Waterloo, Waterloo, ON N2K2E4, Canada (e-mail: dwang@uwaterloo.ca).

Color versions of one or more of the figures in this paper are available online at http://ieeexplore.ieee.org.

Digital Object Identifier 10.1109/TCST.2013.2242329

$$\dot{\boldsymbol{X}}_{\boldsymbol{m_2}} = \bar{\boldsymbol{M}}_{\boldsymbol{m}}{}^{-1}(\boldsymbol{X}_{\boldsymbol{m_1}})\left(-\bar{\boldsymbol{h}}_{\boldsymbol{m}}(\boldsymbol{X}_{\boldsymbol{m_1}}, \boldsymbol{X}_{\boldsymbol{m_2}}) + \boldsymbol{F}_{\boldsymbol{m}} + \boldsymbol{F}_{\boldsymbol{h}}\right) \quad (2)$$

where $\boldsymbol{X}_{\boldsymbol{m_1}} \in R^n$ is the vector of positions and $\boldsymbol{X}_{\boldsymbol{m_2}} \in R^n$ is the vector of velocities. The matrices $\bar{\boldsymbol{M}}_{\boldsymbol{m}}(\boldsymbol{X}_{\boldsymbol{m_1}})$ and $\bar{\boldsymbol{h}}_{\boldsymbol{m}}(\boldsymbol{X}_{\boldsymbol{m_1}}, \boldsymbol{X}_{\boldsymbol{m_2}})$ are defined in [9]. The vectors $\boldsymbol{F}_{\boldsymbol{m}} \in R^n$ and $\boldsymbol{F}_{\boldsymbol{h}} \in R^n$ represent the input forces and the external forces applied by the human, respectively. Defining the slave states similarly, the slave state space representation of the dynamics is given as

$$\dot{\boldsymbol{X}}_{\boldsymbol{s_1}} = \boldsymbol{X}_{\boldsymbol{s_2}} \quad (3)$$

$$\dot{\boldsymbol{X}}_{\boldsymbol{s_2}} = \bar{\boldsymbol{M}}_{\boldsymbol{s}}{}^{-1}(\boldsymbol{X}_{\boldsymbol{s_1}})\left(-\bar{\boldsymbol{h}}_{\boldsymbol{s}}(\boldsymbol{X}_{\boldsymbol{s_1}}, \boldsymbol{X}_{\boldsymbol{s_2}}) + \boldsymbol{F}_{\boldsymbol{s}} - \boldsymbol{F}_{\boldsymbol{e}}\right) \quad (4)$$

where the vectors $\boldsymbol{F}_{\boldsymbol{s}} \in R^n$ and $\boldsymbol{F}_{\boldsymbol{e}} \in R^n$ represent the input forces and the external forces applied by the environment, respectively.

A. Master and Slave Observers

Observers are used at both the master and slave sites. They are based on the observer developed in [10], but are designed for the n-DOF case. They make use of the super-twisting second-order sliding-mode algorithm. For the case of the n-DOF bilateral teleoperation system, multiple-input, multiple-output (MIMO) observers are developed. The observer for the master manipulator is given as

$$\dot{\hat{\boldsymbol{X}}}_{\boldsymbol{m_1}} = \hat{\boldsymbol{X}}_{\boldsymbol{m_2}} + \boldsymbol{z}_{\boldsymbol{m_1}} \quad (5)$$

$$\dot{\hat{\boldsymbol{X}}}_{\boldsymbol{m_2}} = \bar{\boldsymbol{M}}_{\boldsymbol{m}}{}^{-1}(\hat{\boldsymbol{X}}_{\boldsymbol{m_1}})\left(-\bar{\boldsymbol{h}}_{\boldsymbol{m}}(\hat{\boldsymbol{X}}_{\boldsymbol{m_1}}, \hat{\boldsymbol{X}}_{\boldsymbol{m_2}}) + \boldsymbol{F}_{\boldsymbol{m}}\right) + \boldsymbol{z}_{\boldsymbol{m_2}} \quad (6)$$

where $\boldsymbol{z}_{\boldsymbol{m_1}} \in R^n$ and $\boldsymbol{z}_{\boldsymbol{m_2}} \in R^n$. The ith element of vector $\boldsymbol{z}_{\boldsymbol{m_1}}$ is given as

$$z_{m_{1i}} = \lambda_{\mathrm{m_i}} |X_{m_{1i}} - \hat{X}_{m_{1i}}|^{1/2} \mathrm{sign}(X_{m_{1i}} - \hat{X}_{m_{1i}}) \quad (7)$$

and the ith element of vector $\boldsymbol{z}_{\boldsymbol{m_2}}$ is given as

$$z_{m_{2i}} = \alpha_{\mathrm{m_i}} \mathrm{sign}(X_{m_{1i}} - \hat{X}_{m_{1i}}) \quad (8)$$

where $\lambda_{\mathrm{m_i}}$ and $\alpha_{\mathrm{m_i}}$ are constants. Conditions on these constants are given in the Appendix. Note that the human force exerted on the end effector does not appear at all in the observer. Regardless of this, finite time convergence of the state estimates is achieved, and an estimate of the human force is obtained as well. It is this force estimate that is used in the control law. The human force estimate is obtained from the equivalent output injection term $z_{m_{2i}}$ as

$$\hat{\boldsymbol{F}}_{\boldsymbol{h}} = \bar{\boldsymbol{M}}_{\boldsymbol{m}}(\hat{\boldsymbol{X}}_{\boldsymbol{m_1}})\boldsymbol{z}_{\boldsymbol{m_2eq}} \quad (9)$$

where $\boldsymbol{z}_{\boldsymbol{m_2eq}}$ represents a filtering operation on $\boldsymbol{z}_{\boldsymbol{m_2}}$ in order to obtain the equivalent output injection signal [11]. The equations for the slave observer are expressed as

$$\dot{\hat{\boldsymbol{X}}}_{\boldsymbol{s_1}} = \hat{\boldsymbol{X}}_{\boldsymbol{s_2}} + \boldsymbol{z}_{\boldsymbol{s_1}} \quad (10)$$

$$\dot{\hat{\boldsymbol{X}}}_{\boldsymbol{s_2}} = \bar{\boldsymbol{M}}_{\boldsymbol{s}}{}^{-1}(\hat{\boldsymbol{X}}_{\boldsymbol{s_1}})\left(-\bar{\boldsymbol{h}}_{\boldsymbol{s}}(\hat{\boldsymbol{X}}_{\boldsymbol{s_1}}, \hat{\boldsymbol{X}}_{\boldsymbol{s_2}}) + \boldsymbol{F}_{\boldsymbol{s}}\right) + \boldsymbol{z}_{\boldsymbol{s_2}} \quad (11)$$

where $\boldsymbol{z}_{\boldsymbol{s_1}} \in R^n$ and $\boldsymbol{z}_{\boldsymbol{s_2}} \in R^n$. The ith element of vectors $\boldsymbol{z}_{\boldsymbol{s_1}}$ and $\boldsymbol{z}_{\boldsymbol{s_2}}$ are defined analogously to the ith elements of $\boldsymbol{z}_{\boldsymbol{m_1}}$ and $\boldsymbol{z}_{\boldsymbol{m_2}}$, respectively.

The estimate of the environmental force acting on the slave is obtained from the equivalent output injection term $z_{s_2 i}$ as

$$\hat{\boldsymbol{F}}_{\boldsymbol{e}} = -\bar{\boldsymbol{M}}_{\boldsymbol{s}}(\hat{\boldsymbol{X}}_{\boldsymbol{s_1}})\boldsymbol{z}_{\boldsymbol{s_2eq}} \quad (12)$$

where the ith element of vector $\boldsymbol{z}_{\boldsymbol{s_2}}$ is defined analogously to the ith element of $\boldsymbol{z}_{\boldsymbol{m_2}}$, and $\bar{\boldsymbol{M}}_{\boldsymbol{s}}$ is defined analogously to the master. The extension of the single-input, single-output (SISO) observers in [10] to MIMO observers is presented in the Appendix.

B. Control Laws

A signal $\boldsymbol{x}(t)$ delayed by T_1 and T_2 s, respectively, is represented as

$$\boldsymbol{x}^{d_1}(t) \equiv \boldsymbol{x}(t - \mathrm{T}_1),\ \boldsymbol{x}^{d_2}(t) \equiv \boldsymbol{x}(t - \mathrm{T}_2).$$

Similarly, a signal delayed by two time delays, T_1 and T_2, is represented as

$$\boldsymbol{x}^{dd}(t) \equiv \boldsymbol{x}(t - \mathrm{T}_1 - \mathrm{T}_2).$$

The master control law is a computed torque method controller to decouple and linearize each DOF in the task space. The outer loop controller is specified as

$$\boldsymbol{F}_{\boldsymbol{m}} = \bar{\boldsymbol{M}}_{\boldsymbol{m}}(\hat{\boldsymbol{X}}_{\boldsymbol{m_1}})\boldsymbol{v}_{\boldsymbol{m}} + \bar{\boldsymbol{h}}_{\boldsymbol{m}}(\hat{\boldsymbol{X}}_{\boldsymbol{m_1}}, \hat{\boldsymbol{X}}_{\boldsymbol{m_2}}) - \hat{\boldsymbol{F}}_{\boldsymbol{h}}. \quad (13)$$

The inner impedance controller, to provide each degree of freedom with the desired impedance characteristics, is given as

$$\boldsymbol{v}_{\boldsymbol{m}} = \tilde{\mathbf{M}}_m^{-1}\left(-\tilde{\mathbf{B}}_m \hat{\boldsymbol{X}}_{\boldsymbol{m_2}} - \tilde{\mathbf{K}}_m \hat{\boldsymbol{X}}_{\boldsymbol{m_1}} + \hat{\boldsymbol{F}}_{\boldsymbol{h}} - \hat{\boldsymbol{F}}_{\boldsymbol{e}}{}^{d_2}\right) \quad (14)$$

where $\tilde{\mathbf{M}}_m \in R^{n\times n}$ is the diagonal constant matrix that specifies the desired mass characteristic for each degree of freedom. The desired mass for the ith DOF is given by the ith diagonal of $\tilde{\mathbf{M}}_m$. The matrices $\tilde{\mathbf{B}}_m \in R^{n\times n}$ and $\tilde{\mathbf{K}}_m \in R^{n\times n}$ are also diagonal constant matrices representing the desired damping and stiffness values for each DOF.

In order to present the slave controller, define the master-slave position and velocity tracking error as $\boldsymbol{e}_{\boldsymbol{r_1}} = \boldsymbol{X}_{\boldsymbol{s_1}} - \boldsymbol{X}_{\boldsymbol{m_1}}{}^{d_1} \in R^n$ and $\boldsymbol{e}_{\boldsymbol{r_2}} = \boldsymbol{X}_{\boldsymbol{s_2}} - \boldsymbol{X}_{\boldsymbol{m_2}}{}^{d_1} \in R^n$. The controller is designed in order to give each DOF of the end effector a desired impedance characteristic. Controlling the mass, spring, and damping characteristics of the end effector allows the operator to tune the system based on the particular application. The desired impedance model for the slave end effector is expressed as

$$\boldsymbol{Z}_{\boldsymbol{s}}(s) = \frac{\boldsymbol{F}_{\boldsymbol{e}}(s)}{\boldsymbol{V}_{\boldsymbol{e}}(s)} = -\left(\tilde{\mathbf{M}}_s s + \tilde{\mathbf{B}}_s + \frac{\tilde{\mathbf{K}}_s}{s}\right) \quad (15)$$

where $\boldsymbol{F}_{\boldsymbol{e}}(s)$ represents the Laplace transform of the environmental force, $\boldsymbol{V}_{\boldsymbol{e}}(s)$ represents the Laplace transform of the tracking error velocity, and the matrices $\tilde{\mathbf{M}}_s$, $\tilde{\mathbf{B}}_s$, and $\tilde{\mathbf{K}}_s$ are defined as in the master controller, but for the slave impedances. This impedance model gives rise to the following n-DOF equation of dynamics:

$$\boldsymbol{I} = \tilde{\mathbf{M}}_s \dot{\boldsymbol{e}}_{\boldsymbol{r_2}} + \tilde{\mathbf{B}}_s \boldsymbol{e}_{\boldsymbol{r_2}} + \tilde{\mathbf{K}}_s \boldsymbol{e}_{\boldsymbol{r_1}} + \boldsymbol{F}_{\boldsymbol{e}} = 0. \quad (16)$$

This equation is obtained from (15) by taking an inverse Laplace transform. The slave controller is designed to ensure

that the slave closed-loop dynamics have mass, spring, and damping characteristics as specified in (16). Additionally, the controller will ensure that the slave asymptotically tracks the delayed master trajectory in the absence of contact with the environment, with tracking error dynamics given by (16). In order to ensure that this desired impedance characteristic is satisfied, a sliding surface for the slave controller is defined as

$$\boldsymbol{s} = \int_0^t \tilde{\mathbf{M}}_s^{-1} \boldsymbol{I}(\tau)\, d\tau = 0. \tag{17}$$

Once the slave sliding mode controller has driven the system trajectories to $\boldsymbol{s} = 0$, then (16) will be satisfied and the slave manipulator will have the desired closed-loop dynamics. However, this brief examines output feedback control. An output feedback version of the end effector dynamics that yields the desired impedance model is defined as

$$\hat{\boldsymbol{I}} = \tilde{\mathbf{M}}_s \dot{\hat{\boldsymbol{e}}}_{\boldsymbol{r_2}} + \tilde{\mathbf{B}}_s \hat{\boldsymbol{e}}_{\boldsymbol{r_2}} + \tilde{\mathbf{K}}_s \hat{\boldsymbol{e}}_{\boldsymbol{r_1}} + \hat{\boldsymbol{F}}_{\boldsymbol{e}} = 0 \tag{18}$$

where $\hat{\boldsymbol{e}}_{\boldsymbol{r_1}} = \hat{\boldsymbol{X}}_{\boldsymbol{s_1}} - \hat{\boldsymbol{X}}_{\boldsymbol{m_1}}{}^{d_1}$ and $\hat{\boldsymbol{e}}_{\boldsymbol{r_2}} = \hat{\boldsymbol{X}}_{\boldsymbol{s_2}} - \hat{\boldsymbol{X}}_{\boldsymbol{m_2}}{}^{d_1}$. Now, the sliding surface in the output feedback case is defined as

$$\hat{\boldsymbol{s}} = \int_0^t \tilde{\mathbf{M}}_s^{-1} \hat{\boldsymbol{I}}(\tau)\, d\tau = 0. \tag{19}$$

Then, the slave side sliding mode controller is given as

$$\begin{aligned} \boldsymbol{F_s} = -\bar{\boldsymbol{M}}_{\boldsymbol{s}}(\hat{\boldsymbol{X}}_{\boldsymbol{s_1}}) \Big[& \tilde{\mathbf{M}}_s^{-1} \tilde{\mathbf{K}}_s \hat{\boldsymbol{X}}_{\boldsymbol{s_1}} + \tilde{\mathbf{M}}_s^{-1} \tilde{\mathbf{B}}_s \hat{\boldsymbol{X}}_{\boldsymbol{s_2}} \\ & - \bar{\boldsymbol{M}}_{\boldsymbol{s}}{}^{-1}(\hat{\boldsymbol{X}}_{\boldsymbol{s_1}}) \bar{\boldsymbol{h}}_{\boldsymbol{s}}(\hat{\boldsymbol{X}}_{\boldsymbol{s_1}}, \hat{\boldsymbol{X}}_{\boldsymbol{s_2}}) \\ & + (\tilde{\mathbf{M}}_m^{-1} \tilde{\mathbf{K}}_m - \tilde{\mathbf{M}}_s^{-1} \tilde{\mathbf{K}}_s) \hat{\boldsymbol{X}}_{\boldsymbol{m_1}}{}^{d_1} \\ & + (\tilde{\mathbf{M}}_m^{-1} \tilde{\mathbf{B}}_m - \tilde{\mathbf{M}}_s^{-1} \tilde{\mathbf{B}}_s) \hat{\boldsymbol{X}}_{\boldsymbol{m_2}}{}^{d_1} \\ & - (\tilde{\mathbf{M}}_m^{-1} - \bar{\boldsymbol{M}}_{\boldsymbol{m}}{}^{-1}(\hat{\boldsymbol{X}}_{\boldsymbol{m_1}}{}^{d_1})) \hat{\boldsymbol{F}}_{\boldsymbol{h}}{}^{d_1} \\ & + \tilde{\mathbf{M}}_m^{-1} \hat{\boldsymbol{F}}_{\boldsymbol{e}}{}^{dd} + \tilde{\mathbf{M}}_s^{-1} \hat{\boldsymbol{F}}_{\boldsymbol{e}} + \boldsymbol{z}_{\boldsymbol{s_2 eq}} \\ & - \boldsymbol{z}_{\boldsymbol{m_2 eq}}{}^{d_1} + \mathbf{K_g} \mathrm{sign}(\hat{\boldsymbol{s}}) \Big] \end{aligned} \tag{20}$$

where $\mathbf{K_g} = \mathrm{k_g}\mathbf{I} \in R^{n \times n}$ and $\mathrm{k_g}$ is a scalar whose value will be specified later.

To summarize, for master and slave manipulators connected bilaterally through a time delay of $\mathrm{T_1}$ s from the master to the slave and $\mathrm{T_2}$ s from the slave to the master, the system may be controlled using the master control law (13) and (14) with master side observer (5), (6), and slave sliding mode control law (20) with slave side observer (10), (11).

III. Stability of Each of the Master and Slave Plants

In order to show the stability of this system, the following assumption is made.

Assumption 3.1: The external forces acting on both master and slave are bounded for all time with some known upper bounds. In particular, the environment system that generates the forces on the teleoperator is a finite-gain L_2 stable system, and the human dynamics are not considered.

The next theorem shows that the master and slave controllers and observers ensure that each plant has the desired closed-loop dynamics. Additionally, the slave manipulator will asymptotically track the delayed master trajectory.

Theorem 3.1: Consider the master and slave manipulators connected bilaterally through a time delay of $\mathrm{T_1}$ s from the master to the slave and $\mathrm{T_2}$ s from the slave to the master, with master control law (13) and (14), master side observer (5), (6), and slave sliding mode control law (20) with slave side observer (10), (11). Then, there exists a sliding mode controller gain $\mathbf{K_g} = \mathrm{k_g}\mathbf{I}$, where

$$\mathrm{k_g} \geq 2\sqrt{n} \left(\max_i \alpha_{\mathrm{s_i}} + \max_i \alpha_{\mathrm{m_i}} \right) + \varepsilon_{\mathrm{g}} \tag{21}$$

for any $\varepsilon_{\mathrm{g}} > 0$, and observer gains λ_{m}, α_{m}, λ_{s}, α_{s} such that the state estimates recover the true state in finite time, and the master and slave manipulators have the desired closed-loop dynamics.

Proof: See [12]. ■

Theorem 3.1 guarantees stability of each of the master and slave manipulators. The next section addresses the issue of closed-loop stability under a variety of environmental conditions.

IV. Stability of the Teleoperator System in Contact With the Environment

Having guaranteed stability for each of the master and slave manipulators with their associated observers and controllers, it remains to show that the entire closed loop can be stabilized in the presence of time delays. This section will present closed-loop stability results for two situations. The first case looks at the situation where the system may be stabilized for any size of delay, and the delay need not be known *a priori*, provided that the environment is a linear spring damper. The second case presents a delay-dependent stability result for situations involving the same environment at the slave side. Delay-independent stability for nonlinear finite-gain stable environments was presented in [7].

A. Delay-Independent Stability With a Linear Environment

This case examines the situation where the slave end effector is in constant contact with a linear environment. This environment is modeled as a set of n spring-dampers in connection with each DOF of the end effector. The environment is located at $\boldsymbol{X}_{\boldsymbol{s_1}} = \mathbf{X_c}$ and is described by the model

$$\boldsymbol{F}_{\boldsymbol{e}} = \mathbf{K_e}(\boldsymbol{X}_{\boldsymbol{s_1}} - \mathbf{X_c}) + \mathbf{B_e} \boldsymbol{X}_{\boldsymbol{s_2}} \tag{22}$$

where $\mathbf{K_e} \in R^{n \times n}$ is a diagonal matrix of spring constants and $\mathbf{B_e} \in R^{n \times n}$ is a diagonal matrix of damping constants. When this environment is in contact with the slave manipulator, the equilibrium point of the slave system is no longer the origin. In order to perform a stability analysis, a new state is defined to express the slave as a system with an equilibrium at the origin. Define a new state as

$$\boldsymbol{X}_{\boldsymbol{s_1}}{}' = \boldsymbol{X}_{\boldsymbol{s_1}} - \left(\tilde{\mathbf{K}}_s + \mathbf{K_e} \right)^{-1} \mathbf{K_e} \mathbf{X_c}. \tag{23}$$

Applying this transformation to the slave plant ensures that the equilibrium point of the system in the new states is at the origin.

In this section, the Small Gain Theorem is used to develop sufficient conditions to ensure closed-loop stability regardless

of the time delays. A transfer function representation of the master system is used. The master system has as inputs the sum of the human force and the delayed environmental force. Define this input signal as $\boldsymbol{e_1} = \boldsymbol{F_h} - \boldsymbol{F_e}(t - \mathrm{T}_2) \in R^n$. It produces as outputs: position, velocity, and acceleration. Define the master output as $\boldsymbol{Y_m} = [\boldsymbol{X_{m_1}}^T, \boldsymbol{X_{m_2}}^T, \dot{\boldsymbol{X}}_{\boldsymbol{m_2}}^T]^T$. The slave system receives $\boldsymbol{e_2} = \boldsymbol{Y_m}(t - \mathrm{T}_1) \in R^{3n}$ as input. The environmental forces acting on the slave end effector are taken as its output, that is, $\boldsymbol{Y_s} = \mathbf{K_e}\boldsymbol{X_{s_1}}' + \mathbf{B_e}\boldsymbol{X_{s_2}}$. The master transfer function matrix $\boldsymbol{G_m}(s) \in C^{3n \times n}$ can be found as

$$\boldsymbol{G_m}(s) = \begin{bmatrix} \boldsymbol{G_{m_1}}(s) \\ \boldsymbol{G_{m_2}}(s) \\ \boldsymbol{G_{m_3}}(s) \end{bmatrix} \tag{24}$$

where

$$\boldsymbol{G_{m_1}}(s) = \mathrm{diag}\left(\frac{1}{\mathrm{m_{m_i}}s^2 + \mathrm{b_{m_i}}s + \mathrm{k_{m_i}}}\right) \tag{25}$$

$$\boldsymbol{G_{m_2}}(s) = \mathrm{diag}\left(\frac{s}{\mathrm{m_{m_i}}s^2 + \mathrm{b_{m_i}}s + \mathrm{k_{m_i}}}\right) \tag{26}$$

$$\boldsymbol{G_{m_3}}(s) = \mathrm{diag}\left(\frac{s^2}{\mathrm{m_{m_i}}s^2 + \mathrm{b_{m_i}}s + \mathrm{k_{m_i}}}\right) \tag{27}$$

for $i = 1 \ldots n$, where $\mathrm{m_{m_i}}$, $\mathrm{b_{m_i}}$, and $\mathrm{k_{m_i}}$ are the ith diagonals of $\tilde{\mathbf{M}}_m$, $\tilde{\mathbf{B}}_m$, and $\tilde{\mathbf{K}}_m$, respectively. This transfer function matrix takes one input vector, the sum of the applied human force and the delayed slave side force, and has three output vectors—master position, velocity, and acceleration. The time delays in both the feedforward and feedback paths may be combined with each transfer function matrix to yield the following transfer matrices:

$$\boldsymbol{G_m}^{d_1}(s) = \boldsymbol{G_m}(s)e^{-\mathrm{T}_1 s}, \ \boldsymbol{G_s}^{d_2}(s) = \boldsymbol{G_s}(s)e^{-\mathrm{T}_2 s}. \tag{28}$$

Stability of the feedback interconnection of $\boldsymbol{G_m}^{d_1}(s)$ and $\boldsymbol{G_s}^{d_2}(s)$ will now be shown.

Assumption 4.1: An upper bound on the ∞-norm of the slave + environment system $\boldsymbol{G_s}(s)$ is known.

Theorem 4.1: Consider the master system connected through time delays to slave system. Define

$$\gamma_{\mathrm{s+e}} = \frac{1}{||\boldsymbol{G_s}(s)||_\infty}$$

where $||\boldsymbol{G_s}(s)||_\infty$ is the L_2 norm of the slave + environment system. If the master impedance parameters are chosen as

$$\mathrm{m_{m_i}} > \frac{1}{\gamma_{\mathrm{s+e}}}\sqrt{\frac{3}{2}}, \ \mathrm{k_{m_i}} = \mathrm{m_{m_i}}, \ \mathrm{b_{m_i}} = \sqrt{2\mathrm{k_{m_i}}\mathrm{m_{m_i}}} \tag{29}$$

then the closed-loop teleoperator system is L_2 stable, independent of delay.

Proof: See [12]. ∎

B. Delay-Dependent Stability With a Linear Environment

While the results of the previous section show that sufficient conditions may be found to stabilize the closed-loop system for any delay, those choices may be overly conservative for small delays. This section makes use of a result in [13] to determine stability of the closed-loop system for a particular range of delays. That is, for a given choice of the master and slave parameters, the maximum delay for which the system is stable may be found. With this result, the designer may determine if the particular parameters chosen will maintain stability for the delay considered in a particular case.

This result applies for linear systems with commensurate delays. In a teleoperation system, this is achievable as it is always possible to put buffers in the system on each side so that incoming signals may be released to each of the master and slave at a known time interval. In this section, it is assumed that the environment is a linear set of spring-dampers having the form (22).

The theorem from [13] to be presented is valid for linear retarded function differential equation (RFDE) systems of the form

$$\dot{\boldsymbol{x}}(t) = \mathbf{A_0}\boldsymbol{x}(t) + \sum_{k=1}^{\mathrm{m}} \mathbf{A_k}\boldsymbol{x}(t - k\tau), \qquad \tau \geq 0 \tag{30}$$

where $\boldsymbol{x}(t) \in R^n$ and $\mathbf{A_i} \in R^{n \times n}$ for all $i = 0, \ldots, \mathrm{m}$.

The main delay-dependent stability result, found in [13], is now presented.

Theorem 4.2: Suppose that (30) is stable at $\tau = 0$, and let $\mathrm{q} = \mathrm{rank}(\mathbf{A_m})$. Furthermore, define

$$\bar{\tau}_i := \begin{cases} \min_{1 \leq k \leq n} \frac{\theta_k^i}{\omega_k^i} \text{ if } \lambda_i(\boldsymbol{G}(j\omega_k^i), \boldsymbol{H}(j\omega_k^i)) = \\ \qquad e^{-j\theta_k^i} \text{ for some } \omega_k^i \in (0, \infty), \\ \qquad \theta_k^i \in [0, 2\pi] \\ \infty \qquad \text{if } \underline{\rho}(\boldsymbol{G}(j\omega), \boldsymbol{H}(j\omega)) > 1 \\ \qquad \forall \omega \in (0, \infty) \end{cases}$$

where

$$\boldsymbol{G}(s) := \begin{bmatrix} 0 & \mathbf{I} & \cdots & 0 \\ \vdots & \vdots & \ddots & \vdots \\ 0 & 0 & \cdots & \mathbf{I} \\ -(s\mathbf{I} - \mathbf{A_0}) & \mathbf{A_1} & \cdots & \mathbf{A_{m-1}} \end{bmatrix}$$

$$\boldsymbol{H}(s) := \mathrm{diag}(\mathbf{I}, \ldots, \mathbf{I}, -\mathbf{A_m}).$$

Then

$$\bar{\tau} := \min_{1 \leq i \leq q + n(m-1)} \bar{\tau}_i.$$

Equation (30) is stable for all $\tau \in [0, \bar{\tau})$, but becomes unstable at $\tau = \bar{\tau}$.

Note that the notation $\lambda_i(\boldsymbol{A}, \boldsymbol{B})$ represents the ith generalized eigenvalue of two square matrices $\boldsymbol{A}$ and $\boldsymbol{B}$. Also

$$\underline{\rho}(\boldsymbol{A}, \boldsymbol{B}) := \min\{|\lambda| \,|\, \det(\boldsymbol{A} - \lambda\boldsymbol{B}) = 0\}.$$

This theorem requires a frequency sweeping test. Strictly speaking, the theorem requires the evaluation of generalized eigenvalues continuously between 0 rad/s and ∞ rad/s. In practice, a numerical approach is used [13]. The frequency axis is broken up into a grid, and at each grid point the generalized eigenvalues of $\boldsymbol{G}(j\omega_k^i)$ and $\boldsymbol{H}(j\omega_k^i)$ are computed. If $\underline{\rho}(\boldsymbol{G}(j\omega), \boldsymbol{H}(j\omega)) > 1$ for all ω, the system has a delay margin of ∞. If this is not the case, the computation results in pairs (ω_k^i, θ_k^i) that will provide estimates of the delay margin $\bar{\tau}_i$. The smallest $\bar{\tau}_i$ will be the delay margin for the system. The

pairs are found in the cases where the generalized eigenvalues have magnitude one. At these points, the phase θ_k^i is found, since the generalized eigenvalues are complex in general.

To make use of Theorem 4.2 for the bilateral teleoperation system, the closed-loop master and slave dynamics must be expressed as a set of RFDEs of the form (30). Substituting the environment dynamics into the slave dynamics and performing the change of variable (23) to shift the equilibrium of the slave + environment dynamics to the origin yields the following matrices for the RFDE (30) (note that A_0 and A_1 are shown at the bottom of the page):

$$\mathbf{A_2} = \begin{bmatrix} 0 & 0 & 0\ 0 \\ -\tilde{\mathbf{M}}_m^{-1}\mathbf{K_e} & -\tilde{\mathbf{M}}_m^{-1}\mathbf{B_e} & 0\ 0 \\ 0 & 0 & 0\ 0 \\ 0 & 0 & 0\ 0 \end{bmatrix}$$

where the state of the RFDE system is defined as $x(t) = [\boldsymbol{X_{s_1}}'^T, \boldsymbol{X_{s_2}}^T, \boldsymbol{X_{m_1}}^T, \boldsymbol{X_{m_2}}^T]^T$. For n-DOF master and slave manipulators, $\mathbf{A_i} \in R^{4n \times 4n}$ for all $i = 0, \ldots, 2$. In this system, τ represents the delay from the master to the slave and the same delay from the slave to the master. Some terms are delayed by 2τ because the environment force is sent from the slave to the master, and then back from the master to the slave. This accounts for the matrix $\mathbf{A_2}$.

With these matrices defined, the delay-dependent stability of the closed-loop teleoperation system may be checked according to the conditions of Theorem 4.2.

V. Simulation Results

The performance of the algorithm is now examined through a simulation study. The master and slave manipulators are chosen as standard 2-DOF nonlinear serial link manipulators. Both the master and slave have the same dynamic parameters of $\mathrm{m_{m_1}} = \mathrm{m_{m_2}} = \mathrm{m_{s_1}} = \mathrm{m_{s_2}} = 1$ kg for the mass and $l_m = l_s = 1$ m for the length of the links. In this simulation, the desired impedance characteristics for each manipulator are chosen as, $\tilde{\mathbf{M}}_m = 22\mathbf{I}$, $\tilde{\mathbf{B}}_m = 32\mathbf{I}$, $\tilde{\mathbf{K}}_m = 22\mathbf{I}$, $\tilde{\mathbf{M}}_s = \mathbf{I}$, $\tilde{\mathbf{B}}_s = 4\mathbf{I}$, and $\tilde{\mathbf{K}}_s = 4\mathbf{I}$. These values are chosen to ensure that the closed-loop system is stable independent of delay. The master and slave force estimates are obtained with 30-Hz first-order low-pass filters.

The first simulation shows the teleoperation system when the slave is in free motion. The second simulation shows the situation with the slave in contact with an environment, modeled as a linear spring-damper attached to each slave end effector DOF. Time delays of 0.25 s in each direction were used. The system was simulated using a fifth-order Runge–Kutta solver with sample period $\mathrm{T_s} = 10^{-5}$ s to show the ideal performance of the algorithm.

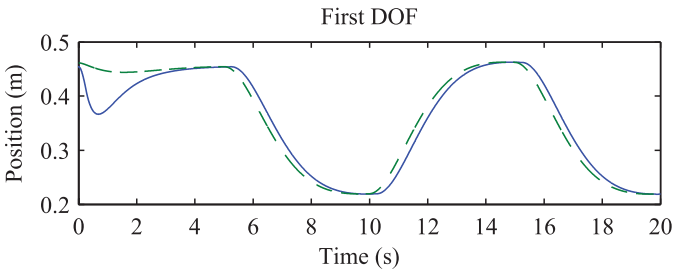

Fig. 1. Position of the slave (solid line) and master (dashed line) end effectors with the slave in free motion.

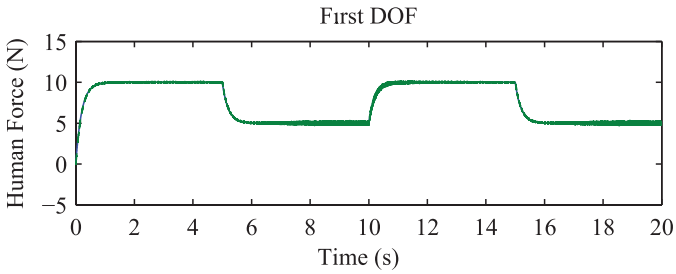

Fig. 2. Actual (solid line) and estimated (dashed line) human force applied to the master manipulator.

A. Simulation Results With Slave in Free Motion

Fig. 1 shows the master and slave end effector trajectories for the first DOF. Signals for the second DOF are similar. The slave manipulator tracks the delayed version of the master trajectory, as desired. Both the master and slave observers perform properly, as expected. The master external force for the first DOF, along with its estimate, is shown in Fig. 2. The external force is estimated quite well. There are some chattering type effects from the switching, but this tends to be no worse than the noise that would be produced from a strain gauge for force sensing.

B. Simulation Results With Slave in Contact

Fig. 3 shows the master and slave end effector positions over time for the first DOF. The results for the second DOF are similar. Due to the definition of the slave desired impedance model, one does not see asymptotic tracking when the slave is in contact with an environment. The slave, when coupled

$$\mathbf{A_0} = \begin{bmatrix} 0 & \mathbf{I} & 0 & 0 \\ -\tilde{\mathbf{M}}_s^{-1}(\tilde{\mathbf{K}}_s + \mathbf{K_e}) & -\tilde{\mathbf{M}}_s^{-1}(\tilde{\mathbf{B}}_s + \mathbf{B_e}) & 0 & 0 \\ 0 & 0 & 0 & \mathbf{I} \\ 0 & 0 & -\tilde{\mathbf{M}}_m^{-1}\tilde{\mathbf{K}}_m & -\tilde{\mathbf{M}}_m^{-1}\tilde{\mathbf{B}}_m \end{bmatrix}$$

$$\mathbf{A_1} = \begin{bmatrix} 0 & 0 & 0 & 0 \\ 0 & 0 & \tilde{\mathbf{M}}_s^{-1}\tilde{\mathbf{K}}_s - \tilde{\mathbf{M}}_m^{-1}\tilde{\mathbf{K}}_m & \tilde{\mathbf{M}}_s^{-1}\tilde{\mathbf{B}}_s - \tilde{\mathbf{M}}_m^{-1}\tilde{\mathbf{B}}_m \\ 0 & 0 & 0 & 0 \\ -\tilde{\mathbf{M}}_m^{-1}\mathbf{K_e} & -\tilde{\mathbf{M}}_m^{-1}\mathbf{B_e} & 0 & 0 \end{bmatrix}$$

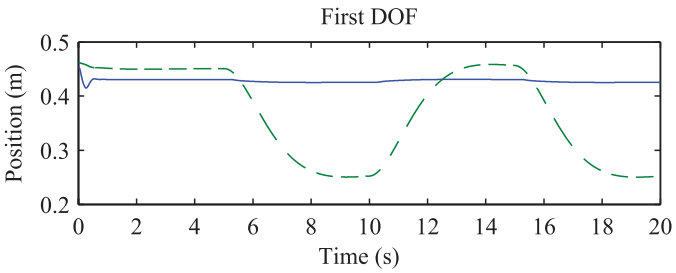

Fig. 3. Position of the slave (solid line) and master (dashed line) end effectors with the slave in contact.

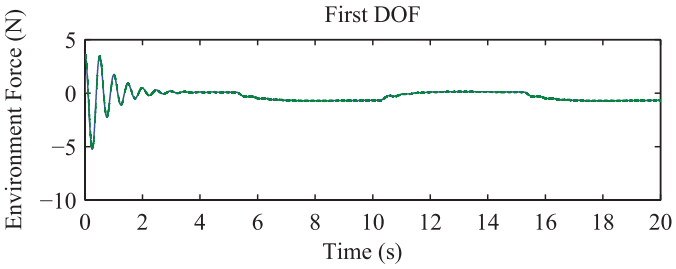

Fig. 4. Actual (solid line) and estimated (dashed line) environment force applied to the slave manipulator.

with the environment, has a much smaller gain than the slave system in free motion. Fig. 4 shows the external environmental force acting on the slave and its estimate for the first DOF. The force estimates are quite accurate.

VI. Experimental Results

The experiments presented in this section validate that the algorithm is practically feasible and has merit as a real-world approach. This algorithm is implemented on two 3-DOF robot manipulators connected to a PC through data acquisition hardware. For each manipulator, the two joints that actuate the five bar linkage were rigidly locked.[1] The base joint of each manipulator was actuated and used as the only degree of freedom in the experiments.

Dynamic models of the base DOF for each manipulator were developed prior to running the experiments. For each robot, the base DOF was modeled as a mass-damper with Coulomb friction. Due to the limitations of the hardware used, the sample time in the experiments is limited to $T_s = 5 \times 10^{-4}$ s. While this sample period is relatively small for the manipulators, it is much larger than the sample period used in simulation. This, along with measurement noise, contributes to more chattering in the sliding mode observer estimates. As a result, the switching components in the observers and the slave controller were replaced by saturation functions to implement boundary layers. The slave control signal was passed through a second-order low-pass filter before being applied to the plant. Without the use of the filter, the chattering became too great, causing too much power draw through the motor amplifier power supply. In order to obtain the estimated force signals from the observers, the switching signals were passed through 5-Hz second-order low-pass filters.

[1]The available hardware permitted only the use of 1 DOF per robot.

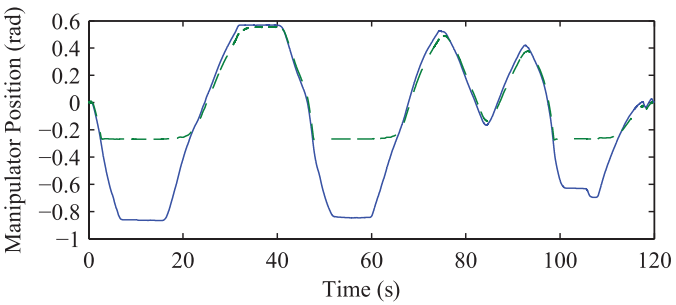

Fig. 5. Position of the master (solid line) and slave (dashed line) manipulators in the first experiment.

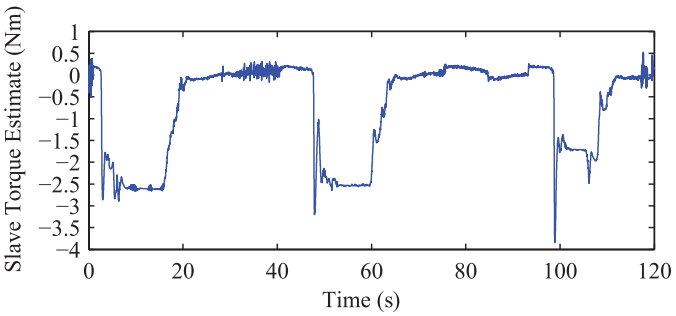

Fig. 6. Estimate of the environmental torque acting on the slave in the first experiment.

For the slave environment, a stiff metal structure was used. Closed-loop impedance parameters were chosen experimentally to ensure stable behavior in contact. A fifth-order Runge–Kutta algorithm was used to integrate the dynamics. The initial experimental run contains no time delays.

In the first experiment, the closed-loop impedance parameters for the master and slave are chosen as $\tilde{M}_m = 7$, $\tilde{B}_m = 14$, $\tilde{K}_m = 0$, $\tilde{M}_s = 7$, $\tilde{B}_s = 14$, and $\tilde{K}_s = 7$. The slave sliding mode controller gain is chosen to be $K_g = 3$. The slave control signal was passed through a linear second-order 100-Hz low pass filter before being applied to the slave manipulator. The environment was placed on the slave side at an angular position of roughly -0.27 rad.

Fig. 5 shows the master and slave positions during the run. As expected, the slave tracks the master when in free motion, but not when in contact with the environment. The estimate of the external torque acting on the slave is given in Fig. 6. This torque estimate is transmitted to the master manipulator, where it can be felt by the operator. When the slave is not in contact with the environment, there is some nonzero torque estimate. This is as a result of running the observers at a relatively large time step as well as the use of boundary layers.

A second experiment was performed, introducing time delays of 0.5 s in each direction. The master closed-loop impedance parameters were chosen as $\tilde{M}_m = 22$, $\tilde{B}_m = 32$, and $\tilde{K}_m = 22$. The slave closed-loop impedance parameters were chosen as $\tilde{M}_s = 7$, $\tilde{B}_s = 42$, and $\tilde{K}_s = 63$. The master impedance parameters were chosen such that the closed-loop system would be stable independent of delay

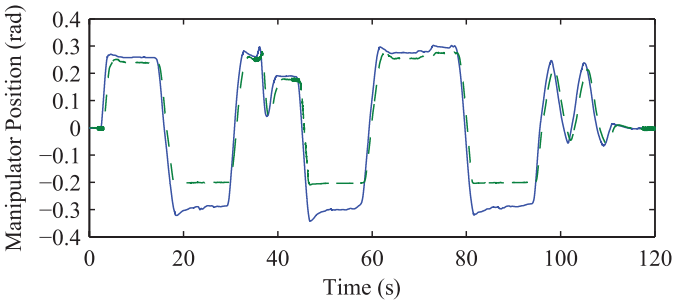

Fig. 7. Position of the master (solid line) and slave (dashed line) manipulators in the second experiment.

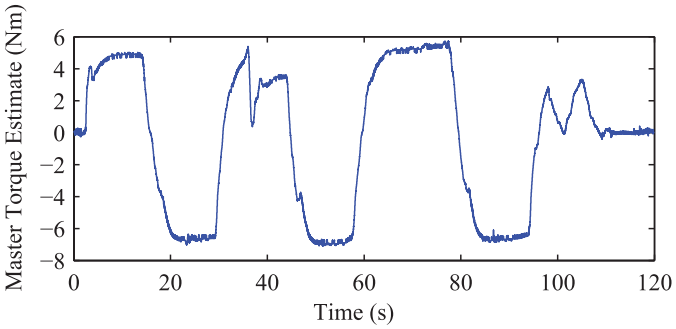

Fig. 8. Estimate of the human torque applied to the master in the second experiment.

by the Small Gain Theorem. The slave control signal was filtered with a second-order low-pass 25-Hz filter. The same environment as the previous experiment was placed on the slave side.

Fig. 7 shows the master and the slave trajectories. The system remains stable both in and out of contact with the environment, and the slave tracks the delayed master trajectory when in free motion. The estimate of the torque applied to the master manipulator is given in Fig. 8. During periods of time when the slave is in contact with the environment, the operator must apply more torque to the master to compensate for the environment torque that is fed back from the slave. This shows the effectiveness of the force feedback portion of the algorithm.

VII. Conclusion

This brief presented a novel bilateral teleoperation algorithm for n-DOF nonlinear manipulators connected through time delays. It provides the benefits of a position-force teleoperation architecture while only requiring position measurements, giving the advantages of both the position-position and position-force architectures while removing their respective disadvantages. By using unknown input sliding mode observers, both the external forces and plant states were estimated exactly with finite time convergence, thus eliminating the need for velocity and force sensors. The output feedback controllers for each of the master and slave decouple and linearize the dynamics in the Cartesian space, allowing one to specify desired impedance characteristics for each end effector DOF.

A theoretical analysis of the observer-controller combinations on each side of the teleoperator has shown stability for each of the manipulators. Closed-loop stability of the whole teleoperator system under time delays was guaranteed for various slave side environments. One avenue for future work on the theoretical development is to perform a closed-loop stability analysis on the system where the assumptions on the human and the environment have been relaxed.

It was found that, in simulation with a sufficiently fast sample frequency, the algorithm performed quite well for cases where the slave is both in and out of contact with an environment. With the use of boundary layers in the slave controller and the observers, as well as with some filtering of the slave control signal, a feasible and practical implementation of this algorithm can be achieved. The experimental results suggested that this algorithm is stable through contact transitions at the slave side. This is one aspect to be examined from a theoretical standpoint in future work. Further future work on this algorithm will examine the use of second-order sliding-mode controllers for the manipulators, thereby eliminating the application of a discontinuous switching signal directly to the plant.

Appendix

The observers used in this brief are based on SISO observers presented in [10]. Here, MIMO observers are designed, and a corollary is developed to prove that the SISO observers may be extended to MIMO observers while still ensuring finite time convergence of the observer error dynamics to zero.

Consider the n-DOF plant

$$\dot{\boldsymbol{x}}_{\boldsymbol{1}} = \boldsymbol{x}_{\boldsymbol{2}} \tag{31}$$

$$\dot{\boldsymbol{x}}_{\boldsymbol{2}} = \boldsymbol{f}(t, \boldsymbol{x}_{\boldsymbol{1}}, \boldsymbol{x}_{\boldsymbol{2}}, \boldsymbol{u}) + \boldsymbol{\xi}(t, \boldsymbol{x}_{\boldsymbol{1}}, \boldsymbol{x}_{\boldsymbol{2}}, \boldsymbol{u}) \tag{32}$$

where $\boldsymbol{x}_{\boldsymbol{1}} \in R^n$, $\boldsymbol{x}_{\boldsymbol{2}} \in R^n$, $\boldsymbol{u} \in R^n$, and $\boldsymbol{y} = \boldsymbol{x}_{\boldsymbol{1}}$. Here, $\boldsymbol{f}(t, \boldsymbol{x}_{\boldsymbol{1}}, \boldsymbol{x}_{\boldsymbol{2}}, \boldsymbol{u})$ represents the known plant dynamics, while $\boldsymbol{\xi}(t, \boldsymbol{x}_{\boldsymbol{1}}, \boldsymbol{x}_{\boldsymbol{2}}, \boldsymbol{u})$ represents the unknown inputs/dynamics. In this case, this term represents the unknown force input. Also, $\boldsymbol{f} \in R^n$ may be expressed as

$$\boldsymbol{f}(t, \boldsymbol{x}_{\boldsymbol{1}}, \boldsymbol{x}_{\boldsymbol{2}}, \boldsymbol{u}) = \begin{bmatrix} f_1(t, \boldsymbol{x}_{\boldsymbol{1}}, \boldsymbol{x}_{\boldsymbol{2}}, \boldsymbol{u}) \\ \vdots \\ f_n(t, \boldsymbol{x}_{\boldsymbol{1}}, \boldsymbol{x}_{\boldsymbol{2}}, \boldsymbol{u}) \end{bmatrix}$$

and equivalently for $\boldsymbol{\xi}(t, \boldsymbol{x}_{\boldsymbol{1}}, \boldsymbol{x}_{\boldsymbol{2}}, \boldsymbol{u}) \in R^n$.

Now consider the following observer for (31) and (32):

$$\dot{\hat{\boldsymbol{x}}}_{\boldsymbol{1}} = \hat{\boldsymbol{x}}_{\boldsymbol{2}} + \boldsymbol{z}_{\boldsymbol{1}} \tag{33}$$

$$\dot{\hat{\boldsymbol{x}}}_{\boldsymbol{2}} = \boldsymbol{f}(t, \boldsymbol{x}_{\boldsymbol{1}}, \hat{\boldsymbol{x}}_{\boldsymbol{2}}, \boldsymbol{u}) + \boldsymbol{z}_{\boldsymbol{2}} \tag{34}$$

where $\hat{\boldsymbol{x}}_{\boldsymbol{1}} \in R^n$ and $\hat{\boldsymbol{x}}_{\boldsymbol{2}} \in R^n$ are the position and velocity estimates. As well, $\boldsymbol{z}_{\boldsymbol{1}} \in R^n$ and $\boldsymbol{z}_{\boldsymbol{2}} \in R^n$. The ith element of vector z_1 is given as

$$z_{1_i} = \lambda_i |x_{1_i} - \hat{x}_{1_i}|^{1/2} \text{sign}(x_{1_i} - \hat{x}_{1_i}) \tag{35}$$

and the ith element of vector z_2 is given as

$$z_{2_i} = \alpha_i \text{sign}(x_{1_i} - \hat{x}_{1_i}). \tag{36}$$

It is assumed that $\hat{\boldsymbol{x}}_{\boldsymbol{1}}(0) = \boldsymbol{x}_{\boldsymbol{1}}(0)$ and $\hat{\boldsymbol{x}}_{\boldsymbol{2}}(0) = 0$. Now define the term $F(t, \boldsymbol{x_1}, \boldsymbol{x_2}, \hat{\boldsymbol{x}}_{\boldsymbol{2}}, \boldsymbol{u}) \in R^n$ as

$$\boldsymbol{F}(t, \boldsymbol{x_1}, \boldsymbol{x_2}, \hat{\boldsymbol{x}}_{\boldsymbol{2}}, \boldsymbol{u}) = \boldsymbol{f}(t, \boldsymbol{x_1}, \boldsymbol{x_2}, \boldsymbol{u}) - \boldsymbol{f}(t, \boldsymbol{x_1}, \hat{\boldsymbol{x}}_{\boldsymbol{2}}, \boldsymbol{u}) + \boldsymbol{\xi}(t, \boldsymbol{x_1}, \boldsymbol{x_2}, \boldsymbol{u}) \tag{37}$$

and assume that the inequality

$$|F_i(t, \boldsymbol{x_1}, \boldsymbol{x_2}, \hat{\boldsymbol{x}}_{\boldsymbol{2}}, \boldsymbol{u})| < \mathrm{f}_\mathrm{i}^+ \tag{38}$$

holds over the operational domain. Provided that the plant being stabilized does not have a finite escape time and the controller that has been designed will stabilize the plant in the full-state feedback case, one may choose the observer dynamics to be fast enough so that the state estimates are recovered before the plant trajectories leave some chosen area [10]. Let α_i and λ_i satisfy the following inequalities, for every element i:

$$\alpha_\mathrm{i} > \mathrm{f}_\mathrm{i}^+ \tag{39}$$

$$\lambda_\mathrm{i} > \sqrt{\frac{2}{\alpha_\mathrm{i} - \mathrm{f}_\mathrm{i}^+}} \frac{(\alpha_\mathrm{i} + \mathrm{f}_\mathrm{i}^+)(1 + \mathrm{p_i})}{(1 - \mathrm{p_i})}. \tag{40}$$

where $\mathrm{p_i}$ is some chosen constant such that $0 < \mathrm{p_i} < 1$. Then, one can state the following corollary.

Corollary 7.1: Suppose that the parameters for the observer (33) and (34) are selected according to the above conditions (39) and (40) for α and λ, and that condition (38) holds over the operational domain of the plant. Then, the variables of the observer converge in finite time to the states of the system, i.e., $(\hat{\boldsymbol{x}}_{\boldsymbol{1}}, \hat{\boldsymbol{x}}_{\boldsymbol{2}}) \rightarrow (\boldsymbol{x_1}, \boldsymbol{x_2})$. Further, the ith component of the unknown vector $\boldsymbol{\xi}(t, \boldsymbol{x_1}, \boldsymbol{x_2}, \boldsymbol{u})$ may be recovered in finite time as $\alpha_\mathrm{i} \operatorname{sign}(x_{1_i} - \hat{x}_{1_i})_{\mathrm{eq}}$.

Proof: See [12]. ■

REFERENCES

[1] D. A. Lawrence, "Stability and transparency in bilateral teleoperation," *IEEE Trans. Robot. Autom.*, vol. 9, no. 5, pp. 624–637, Oct. 1993.

[2] G. Niemeyer and J.-J. E. Slotine, "Telemanipulation with time delays," *Int. J. Robot. Res.*, vol. 23, pp. 873–890, Sep. 2004.

[3] M. Tavakoli, A. Aziminejad, R. V. Patel, and M. Moallem, "Enhanced transparency in haptics-based master-slave systems," in *Proc. Amer. Control Conf.*, Jul. 2007, pp. 1455–1460.

[4] I. Polushin, P. Liu, C. Lung, and G. On, "Position-error based schemes for bilateral teleoperation with time delay: Theory and experiments," *J. Dynamic Syst., Meas., Control*, vol. 132, no. 3, pp. 031008-1–031008-11, 2010.

[5] L. G. Garcia-Valdovinos, V. Parra-Vega, and M. A. Arteaga, "Observer-based higher-order sliding mode impedance control of bilateral teleoperation under constant unknown time delay," in *Proc. IEEE/RSJ Int. Conf. Intell. Robot. Syst.*, Oct. 2006, pp. 1692–1699.

[6] J. M. Daly and D. W. L. Wang, "Bilateral teleoperation using unknown input observers for force estimation," in *Proc. Amer. Control Conf.*, Jun. 2009, pp. 89–95.

[7] J. M. Daly and D. W. L. Wang, "Time-delayed bilateral teleoperation with force estimation for n-dof nonlinear robot manipulators," in *Proc. IEEE/RSJ Int. Conf. Intell. Robot. Syst.*, Oct. 2010, pp. 3911–3918.

[8] H. C. Cho, J. H. Park, K. Kim, and J.-O. Park, "Sliding-mode-based impedance controller for bilateral teleoperation under varying time delay," in *Proc. IEEE Int. Conf. Robot. Autom.*, Apr. 2001, pp. 1025–1030.

[9] M. W. Spong and M. Vidyasagar, *Robot Dynamics and Control*. New York, USA: Wiley, 1989.

[10] J. Davila, L. Fridman, and A. Levant, "Second-order sliding-mode observer for mechanical systems," *IEEE Trans. Autom. Control*, vol. 50, no. 11, pp. 1785–1789, Nov. 2005.

[11] S. Drakunov and V. Utkin, "Sliding mode observers. tutorial." in *Proc. 34th Conf. Decision Control*, Dec. 1995, pp. 3376–3378.

[12] J. M. Daly, "Output feedback bilateral teleoperation with force estimation in the presence of time delays," Ph.D. dissertation, Dept. Comput. Sci., Univ. Waterloo, Waterloo, ON, Canada, Apr. 2010.

[13] K. Gu, V. L. Kharitonov, and J. Chen, *Stability of Time-Delay Systems*. New York, USA: Birkhauser, 2003.